



Co-deposition of Ni-Co alloys on carbon steel and corrosion resistance

I. Kharmachi^{1,2}, L. Dhouibi¹, P. Berçot², M. Rezrazi²

¹Unité de recherche Mécanique-Energétique, Equipe Corrosion et Protection des Métalliques, ENIT, Université de TunisEl-Manar, BP 37, Tunis Belvédère, 1002, Tunisia

²Institut UTINAM, CNRS UMR 6213, Université de Franche-Comté, 16 route de Gray, 25030 Besançon Cedex, France

Received 25 Jan 2015, Revised 12 May 2015, Accepted 12 May 2015

*Corresponding Author. E-mail adress : imen.kharmachi@univ-fcomte.fr; Tel.: (+21696477524)

Abstract

Ni-Co alloys were synthesized on carbon steel by electrodeposition method using electrolytes with different Ni²⁺ concentrations. The co-deposition phenomenon of Ni-Co alloys was described as anomalous behavior. Morphology and microstructure were investigated by scanning electron microscope and XRD analysis and correlated with Ni/Co ratio in plating bath. Both granular crystals and smooth surface morphology were illustrated with SEM micrographs, and a combination of fcc and hcp structure were characterized by XRD patterns which depended strongly on cobalt content in the deposit. The electrochemical properties of Ni-Co alloy coatings were evaluated in 3% NaCl solution by means of potentiodynamic polarization and electrochemical impedance spectroscopy (EIS). A better corrosion resistance was obtained with rich nickel deposit.

Keywords: Ni-Co alloys, electrodeposition, anomalous behavior, electrochemical properties, corrosion resistance.

1. Introduction

The study of metallic coatings and their functional properties have been an important subject for scientists during the last two decades. This has been attributed to novel mechanical, magnetic and catalytic properties and corrosion resistance for these materials [1-2]. These alloys are important and have been produced by various techniques including physical vapor deposition, chemical or electroless plating and electrodeposition [3]. The alloys produced by electrodeposition include Ni-Co alloy. The electrodeposition of Ni-Co is shown by many researchers as anomalous codeposition [4]; this phenomenon means that the less noble metal (Co) is preferentially deposited. Fan and Piron [5] studied the electrochemical deposition of Ni-Co alloys in various baths and according to Renata Orinakova et.al. [6], the anomalous behavior only occurred at current densities lower than 100 mA cm⁻² in the chloride bath. The properties of Ni-Co alloys depend strongly on cobalt content. The amount of cobalt in the Ni-Co deposit can be controlled by experimental parameters, such as electrolyte composition, pH, stirring, temperature, deposition potential or current, etc [7-8]. The changing of deposition conditions can modify the metal content in the deposit, morphology and microstructure of Ni-Co alloy. The purpose of this work is to study the influence of electrolyte composition on the surface morphology, the chemical content of binary alloys and the corrosion resistance as well as some other properties.

2. Experimental

2.1. Electrodeposition process

The composition of basic plating bath of Ni-Co alloys deposition was shown in **Table 1** [9]. In order to investigate the effect of electrolyte composition in electrodeposits Ni-Co, the electrodeposition was carried out in solutions containing different ratio $R = \frac{[Ni^{2+}]}{[Co^{2+}]}$ in the bath. All experiments were repeated, and no significant difference was found in results obtained under identical conditions.

Table 1 Electrolyte composition and deposition conditions for Ni-Co binary coatings.

Bath composition	Concentration(g L ⁻¹)	Plating parameters	R= $\frac{[Ni^{2+}]}{[Co^{2+}]}$ in bath
NiSO ₄ .6H ₂ O	[6, 60, 180, 300]	pH=2±0.2 Temperature (°C): 25±2	[1, 10, 30, 50]
CoSO ₄ .7H ₂ O	6		
H ₃ BO ₃	40		
Saccharin	3		

Low carbon steel panels with plated area of 0.2 cm² was used to perform galvanostatic measurements. The chemical composition of the steel cathode (STUB 100CR6) was 0.45% C, 1.5% Mn, 0.45% Si and 0.06% S (wt.%). The steel substrates were polished with SiC grinding paper (SiC #500, #800, #1200, #2400), cleaned with acetone using ultrasonics-cleaning equipment for 2 min, and then rinsed with distilled water and the pH value of plating bath was adjusted with H₂SO₄ to 2±0.2. In addition, the depositions were carried out in fresh solutions at 25 ± 2°C without using agitation and at current density of 25 mA cm⁻².

2.2. Electrochemical measurements

A 3-electrode cell was used to conduct the electrochemical experiments. The counter electrode was platinum with an area of 1cm² and the reference electrode was a saturated calomel SCE (Hg/Hg₂Cl₂/KCl) and the working electrode was a coated sample used for potentiodynamic measurements. The coated sample was exposed to 3 % NaCl solution and potentiodynamic polarization studies and electrochemical impedance spectroscopy (EIS) were used to study the corrosion behavior of Co-Ni alloy coatings. These measurements were performed respectively with potentiostat PGP 401 and interface solartron SI 1287/SI 1250. The measurements were performed at room temperature and free air conditions. Prior to the studies the sample was immersed in the corrosive medium for 1 hour to attain open circuit potential (E_{ocp}) or the steady state potential. After the stabilization of the open circuit potential, the upper and the lower potential limits were fixed to ±250 mV with respect to E_{ocp} and the scan rate used was 0.5 mV/s for carrying out the potentiodynamic polarization studies. Impedance measurement was conducted in the frequency range of 100 kHz to 10 mHz and an amplitude of 10 mV was applied on the open circuit potential.

2.3. Characterization studies

The cobalt and nickel content in the deposit was determined using X-ray spectrometer -FISCHERSCOPE X-ray system XDAL series, model FISHER equipped with energy dispersive X-rays analysis (EDX), which was working at 15 kV affiliated with the scanning electron microscope. The surface morphology of the deposits was followed with A JEOL 5410 LV. The crystal orientation was determined using an X-ray diffractometer D8 (Advance Bruker) equipped with a copper anode generating Ni-filtered employing CuK α radiation of wavelength 0.154 nm. The crystallite size of Co-Ni coating was determined, applying line broadening technique using Scherrer equation [10], $D = K\lambda / \beta \cos\theta$ where, K is the Scherrer factor ≈ 1 , D is the crystallite size, λ is the incident radiation wavelength, β is the integral breadth of the structurally broadened profile and θ is the angular position.

3. Results and discussion

3.1. Electrodeposition process and FRX analysis

The electrodeposition was carried out at room temperature, on carbon steel substrate and after immersion of 30 min, the concentrations of cobalt sulfate CoSO₄.7H₂O, boric acid H₃BO₃ and saccharin C₆H₄SO₃NH were fixed respectively at 6 g L⁻¹, 40g L⁻¹ and 3 g L⁻¹, but nickel sulfate concentration was changed in order to obtain a ratio R in the bath that varied from 1 to 50. The X-ray fluorescence results are presented in **Table 2**. As shown in the table, the cobalt content in the deposit increased gradually from 9 wt.% to 53 wt.% when the bath ratio $R = \frac{[Ni^{2+}]}{[Co^{2+}]}$ was decreased from 50 to 1. The Co content of the film depends on the percentage of cobalt in electrolyte.

Fig. 1 showed that the percentage of Co in the film was higher than the percentage in the electrolyte. Several studies have been put in literature to understand the phenomenon. This refers to anomalous behavior of nickel and cobalt ions that was studied by Brenner [11]. He has explained anomalous codeposition of binary alloys of the iron group metals as the member that shows retardation of discharge in codeposition is the one that normally

deposits with the higher over voltage. Some researchers have proposed electrodeposition mechanism which characterized by the rise of pH at the cathode.

Table 2 The data obtained from compositional measurements

Ni concentration (g L ⁻¹)	R ratio in bath	FRX analysis	
		Co (wt.%)	Ni (wt.%)
300	50	9	91
180	30	12	88
60	10	27	73
6	1	53	47

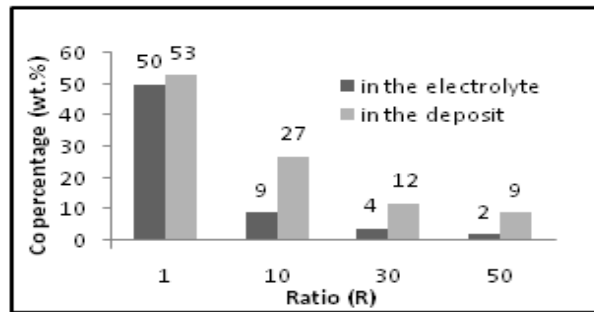


Fig. 1. The variation of cobalt content in the deposit with different ratio in the electrolyte

This local increase in pH caused by the precipitation of metal hydroxides on the cathode, the deposition process occurs in several steps based on adsorption of metal hydroxyl ions on the deposits Eq.(1,2):



Where M represents Co or Ni atoms.

The OH⁻ ion formed at the end of the reaction favors the formation of MOH⁺ and enhances the adsorption of MOH⁺. The adsorption ability of Co(OH)⁺ was considered to be higher than Ni(OH)⁺ this can cause enriching of binary alloy with less noble metal (Co).

3.2. Surface morphology of Ni-Co alloys

Fig. 2 showed the surface morphology of Ni-Co films deposited on carbon steel substrate with different Co content in the coating. With a low percentage of Co in the deposit (up to 30 wt.%) a smooth surface can be observed as seen in **Fig. 2**. But when the Co content was increased to 53 wt.%, the surface morphology became granular related to nucleation and growth mechanism.

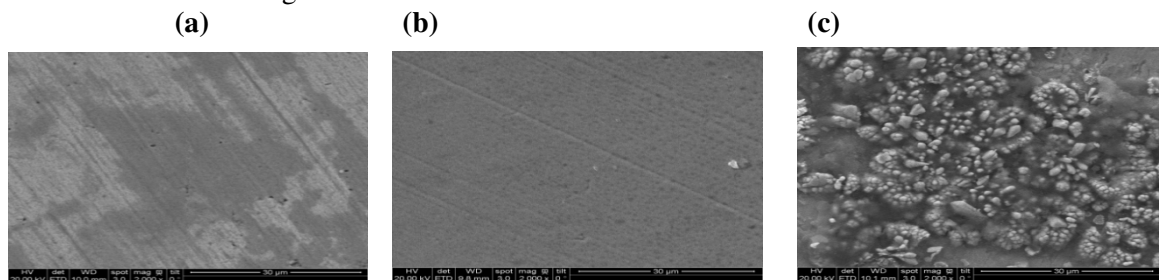


Fig. 2. SEM micrographs of the surfaces of Ni-Co coated steel in plating baths with different Co content in the deposit, (a) 9 wt.% Co, (b) 27 wt.% Co, (c) 53 wt.% Co.

3.3. XRD analysis

Fig. 3 Presented the XRD patterns of Ni-Co coatings deposited on carbon steel substrate from the electrolyte containing different concentrations of Ni²⁺.

The binary Ni-Co phase diagram [13] indicates that the structure consists of α phase, which is a substitutional solid solution of Ni and Co and the structure was face centered cubic (fcc). In this study, the fcc peaks were observed in all XRD patterns. For plain nickel and up to Ni-30wt.% Co alloys (Fig. 3.a-b-c), the structure was found to be fcc with the predominance of (111) orientation.

Refer to many studies [14, 15], when the Co content increase to Ni-50wt.% Co alloy, fcc phase turned to a mixed crystalline structure of fcc and hcp.

This mixed cell structure is composed of α phase along with the presence of a peritectic phase [14]. The peritectic phase is a combination of fcc and hcp cellular system. The increase of cobalt amount to 100wt.% Co in the alloy results the predominance of complete hcp crystal structure which is the similar structure of plain cobalt deposit.

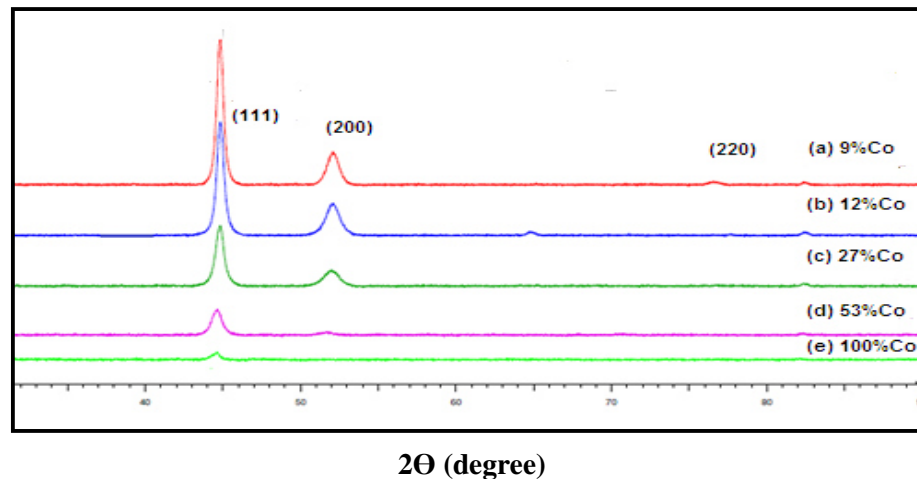


Fig. 3. XRD patterns of Ni-Co binary coatings deposited from the electrolyte (25 mA cm^{-2} , 30 min, pH=2) with different Co content in the deposit, (a) 9 wt.% Co, (b) 12 wt.% Co, (c) 27 wt.% Co, (d) 53 wt.% Co, (e) 100 wt.% Co

3.4. Corrosion characterization of Ni-Co alloys

3.4.1. Potentiodynamic polarization studies

The corrosion parameters such as corrosion potential (E_{corr}), corrosion current density (i_{corr}), cathodic (bc) and anodic (ba) Tafel slope are calculated by using Tafel fit. The Tafel plot, i.e. $\log i$ vs. E obtained from polarization studies (Fig. 4).

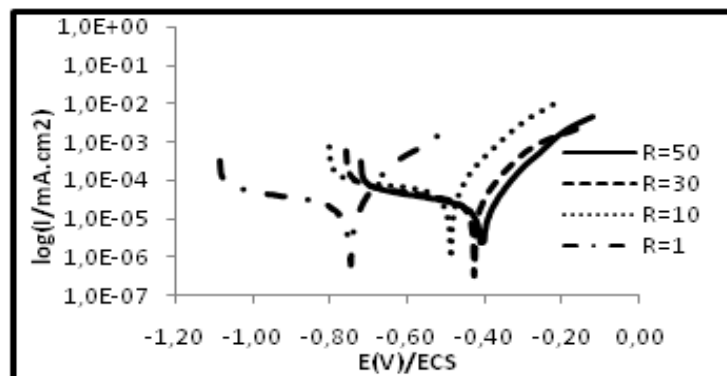


Fig. 4. Polarization curves in 3% sodium chloride of Ni-Co alloy coatings electrodeposited on carbon steel substrate with different ratio in the electrolyte

E_{corr} shifted toward more positive values with high ratio in the electrolyte (R=50) which was related to the low percentage of cobalt in the deposit (Ni-9wt.%Co)(Table 3). However, the i_{corr} value was decreased. So, a better

corrosion resistance was obtained with rich nickel deposit. This result was confirmed with polarization resistance value (R_p) that was found to be the highest for (Ni-9wt.% Co) coating.

Table 3 Potentiodynamic polarization data of Ni-Co alloys

Ratio in electrolyte $R = \frac{[Ni^{2+}]}{[Co^{2+}]}$	E_{corr} (mV)	i_{corr} (mA cm ⁻²)	ba (mV dec ⁻¹)	-bc (mV dec ⁻¹)	R_p (Ω cm ²)
1	-750	0,31	84	880	108
10	-555	0,25	77	430	161
30	-451	0,08	80	250	321
50	-399	0,04	88	185	1940

3.4.2. Electrochemical impedance spectroscopy (EIS) studies

Electrochemical impedance spectroscopy (EIS) was exploited in order to evaluate the corrosion behavior of Ni-Co coatings after one hour of immersion in 3% NaCl solution (pH= 7.2) at 25°C. The Nyquist diagrams were presented in Fig. 5 for Ni-Co alloys prepared in baths with different ratio $R = \frac{[Ni^{2+}]}{[Co^{2+}]}$. In this complex-plane representation, three semicircles were generally observed.

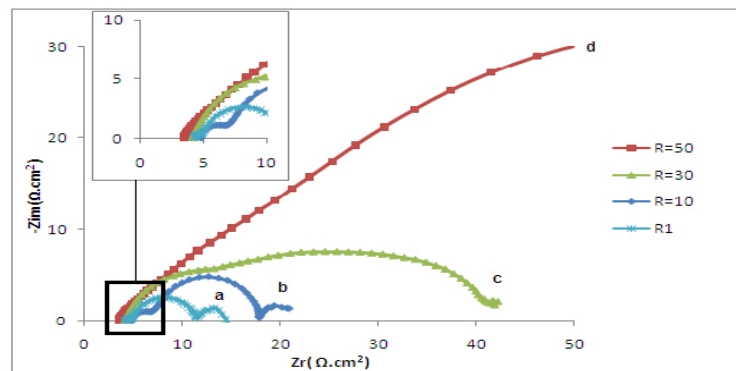


Fig. 5. Nyquist plot of Ni-Co coatings electrodeposited on carbon steel substrate with different ratio $R = \frac{[Ni^{2+}]}{[Co^{2+}]}$. (a) R=1, (b) R=10, (c) R=30, (d) R=50

Table 4 Data obtained by electrochemical impedance spectroscopy of coatings immersed in 3% NaCl solution

Ratio in electrolyte $R = \frac{[Ni^{2+}]}{[Co^{2+}]}$	R_c (Ω cm ²)	R_{pc} (Ω cm ²)	C_c (F cm ⁻²)	R_t (Ω cm ²)	C_{dl} (F cm ⁻²)	R_F (Ω cm ²)	C_F (F cm ⁻²)
1	4,3	0,01	$1,6 \cdot 10^{-5}$	6	$1,5 \cdot 10^{-4}$	3	1,3
10	4,9	2,6	$3,1 \cdot 10^{-5}$	10	$0,6 \cdot 10^{-4}$	34	1,5
30	4,4	9,8	$8,6 \cdot 10^{-5}$	13	$0,08 \cdot 10^{-4}$	14	0,01
50	3,8	7,2	$5,32 \cdot 10^{-5}$	27	$0,3 \cdot 10^{-4}$	73	0,002

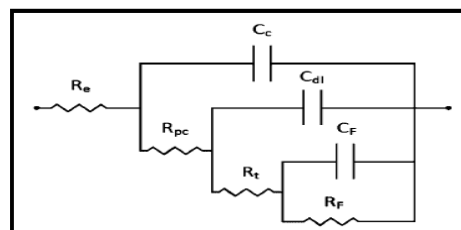


Fig. 6. Equivalent circuit used for Co-Ni-coated carbon steel to fit the impedance data

Fig. 6 showed the equivalent circuit with three RC components was used to interpret the response of the Ni-Co system. The first time constant (R_{pc} , C_c) was attributed to the protective coating properties, (R_i , C_{dl}) an intermediate relaxation in which R_i was the charge transfer resistance of the corrosive process and C_{dl} was the double layer capacitance at the interface.

This time constant was probably due to the heterogeneity of the film which can result from the existence of high and low density zones inside the film [16]. The third time constant (R_F , C_F) in the low frequency part could be attributed to the deposited corrosion products. In all cases, the proposed model was in total agreement with the experimental data. Nyquist diagrams showed that the impedance modulus of the samples rose with increasing of the ratio in the electrolyte.

The R_i and R_{pc} values found for Ni-Co system increased with the increasing of the ratio R from 1 to 50 which related also to the decrease of the amount of cobalt. The corrosion resistance was high for an important value of ratio $R = \frac{[Ni^{2+}]}{[Co^{2+}]}$ obviously, demonstrated with nickel-rich deposits would be superior compared to the other coatings and bad corrosion behavior is observed with the rising of cobalt content.

4. Conclusion

Ni-Co coatings were electrodeposited on carbon steel substrates from electrolyte with different ratio of Ni^{2+} and Co^{2+} that varying from 1 to 50. The content of cobalt had a great effect on the microstructure, surface morphology, microhardness and corrosion properties. The compositions studied showed anomalous codeposition which was characterized by a percentage of cobalt in the deposit higher than Co in bath. Moreover, the morphology was modified from smooth surface to granular structure.

The XRD data revealed the coexistence of two phases: fcc phase for rich nickel deposit (up to 50wt.% Co) and hexagonal hcp for rich cobalt coatings. The corrosion behavior of Ni-Co alloy coatings was evaluated by means of potentiodynamic polarization and electrochemical impedance spectroscopy (EIS) studies and a better corrosion resistance was obtained with rich nickel deposit (Ni-9wt.% Co). This result can be deduced from corrosion parameters obtained from Tafel plot and the Nyquist diagrams. As a conclusion, a coating with important amount of cobalt is less protective to carbon steel substrate than another with more nickel content.

Acknowledgments - The authors would like to acknowledge the financial support provided by "Action Intégrée Franco-Tunisienne du Ministère des Affaires Etrangères et Européennes français et du Ministère de l'Enseignement Supérieur, de la Recherche Scientifique et de la Technologie tunisien".

References

1. Mehmood M, Akiyama E, Habazaki. H, Kawashima A, Asami K and Hashimoto K, *Corros. Sci.*, 42 (2000) 361.
2. Souza C. A. C, May J. E, Carlos I. A, de Oliveira M. F, Kuri S. E, Kiminami C. S. J, *Non-Cryst. Solids*, 304 (2002) 210.
3. Darkowski A, *Surf. Coat. Tech.*, 30 (1987) 131.
4. Dolati A, Sababi M, Nouri E, Ghorbani M, *Materials Chem. Phys.*, 102 (2007) 118.
5. Fan C, Piron D.L *Electrochem. Acta* 41 (1996) 1713.
6. Orinakova R, Orinak A, Vering G, Talian I, Smith R, Arlinghaus H, *Thin, Solid, Films*, 516 (2008) 3045.
7. Abner Brenner, *Electrodeposition of alloys, Principles and Practice*, Vol. II, Academic Press.
8. Golodnitsky D, Gudin N.V, Volyanuk G.A, *Plating Surf. Finish*, 2 (1998) 65.
9. Yundong Li, Hui Jiang, Weihua Huang, Hui Tian, *Appl. Surf. Sci.*, 254 (2008) 6865.
10. Gyftou P, stroumbouli M, Pavlatou E.A, Asimidis P, Spyrellis N, *Electrochim. Acta* 50 (2005) 4544.
11. Grigoryan N.S, Kudryavtsev V.N, Zhdan P.A, kolotyrkin I.V, Volynskaya E.A, *Zasch. Met.* 25 (1989) 288.
12. Liangliang Tian, Jincheng Xu, Songtao Xiao, *Vacuum*, 86 (2011) 27.
13. Malone G.A, Winkelman D.M *High Performance Alloy Electroforming Final Report*, Report No.8874-927001
14. Srivastava M, Selvi V.E, Grips V.K.W, Rajam K.S, *Surf. Coat. Technol.*, 201 (2006) 3051.
15. Wang L, Gao Y, Xue Q, Liu H, Xu T, *Appl. Surf. Sci.*, 242 (2005) 326.
16. Durairajan A, Haran B.S, White R.E, Popov B.N, *J. Electrochem. Soc.*, 5 (2000) 147.

(2015) ; <http://www.jmaterenvirosci.com>